

Article

Performance Evaluation of Asphalt Modified with Steel Slag Powder and Waste Tire Rubber Compounds

Zipeng Wang¹, Zenggang Zhao^{2,*}, Chao Yang² , Xinkui Yang², Shuaichao Chen² and Yingxue Zou²

¹ Key Laboratory of Road and Traffic Engineering of the Ministry of Education, Tongji University, Shanghai 201804, China; wangzipeng_sjz@126.com

² State Key Laboratory of Silicate Materials for Architectures, Wuhan University of Technology, Wuhan 430070, China; hbyangc@whut.edu.cn (C.Y.); yangxk@whut.edu.cn (X.Y.); chensc@whut.edu.cn (S.C.); zouyingxue@whut.edu.cn (Y.Z.)

* Correspondence: zhaozenggang@whut.edu.cn

Abstract: As two kinds of solid wastes, waste tires and steel slag have caused serious threats to the environment. Both waste tire rubber (WTR) and steel slag powder (SSP) can improve the performance of asphalt, while the performance indexes and modification mechanism of modified asphalt are not clear. In this paper, asphalt modified with SSP and WTR was prepared, and its performance was evaluated. The physical properties of asphalt modified with SSP and WTR, including penetration, the softening point, and viscosity, were investigated. Furthermore, high-temperature performance, fatigue resistance, low-temperature performance, and blending mechanism of asphalt modified with SSP and WTR were tested with a dynamic shear rheometer (DSR), bending beam rheometer (BBR), and Fourier transform infrared spectrometer (FTIR). The results showed that with the same content of WTR and SSP, WTR reveals a more significant modification effect on physical properties, fatigue, and low-temperature performance of base asphalt than SSP. The anti-rutting performance of SSP-modified asphalt is better than that of WTR-modified asphalt at 30–42 °C, and the anti-rutting performance of WTR-modified asphalt is better than that of SSP-modified asphalt at 42–80 °C. When the total content of WTR and SSP is the same, the physical properties, high-temperature resistance, fatigue resistance, and low-temperature performance of the asphalt modified with WTR and SSP decrease with the decrease in the ratio of WTR and SSP, and their performance is between WTR-modified asphalt and SSP-modified asphalt. Infrared spectrum results verified that the preparation of WTR- and SSP-modified asphalt is mainly a physical blending process. Overall, this research is conducive to promoting the application of modified asphalt with WTR and SSP in the construction of high-standard pavement.



Citation: Wang, Z.; Zhao, Z.; Yang, C.; Yang, X.; Chen, S.; Zou, Y. Performance Evaluation of Asphalt Modified with Steel Slag Powder and Waste Tire Rubber Compounds. *Sustainability* **2022**, *14*, 8615. <https://doi.org/10.3390/su14148615>

Academic Editor: Dimitrios Komilis

Received: 14 June 2022

Accepted: 12 July 2022

Published: 14 July 2022

Publisher's Note: MDPI stays neutral with regard to jurisdictional claims in published maps and institutional affiliations.



Copyright: © 2022 by the authors. Licensee MDPI, Basel, Switzerland. This article is an open access article distributed under the terms and conditions of the Creative Commons Attribution (CC BY) license (<https://creativecommons.org/licenses/by/4.0/>).

Keywords: compound-modified asphalt; waste tire rubber; steel slag powder; physical properties; rheological properties

1. Introduction

As the construction of highways develops rapidly, asphalt pavement has become the main form of high-grade pavement engineering [1,2]. Nevertheless, the rapid growth of traffic volume and serious overloading make asphalt pavements face severe challenges. The asphalt pavement of many expressways cannot meet the needs of traffic soon after it is built, and early damage occurs [3]. The performance of asphalt directly affects the pavement performance of the asphalt mixture and the service condition of pavement [3]. To improve the service quality and service life of asphalt pavement, researchers have prepared mixtures by using modified asphalt that can enhance the road performance of an asphalt mixture [4–7].

Waste tires are a kind of solid waste that has caused serious threats to the environment [8–10]. Road researchers can solve this problem by using waste tire and steel slag

separately for road engineering. Many studies have demonstrated that crumb-rubber-modified asphalt has outstanding elasticity and fatigue resistance [11,12]. Waste tires are first crushed into crumb rubber, and then the asphalt mixture is prepared by dry and wet methods. In the wet method, rubber and asphalt are first turned into rubber-modified asphalt, and then the rubber-asphalt is used as a binder to prepare a rubberized asphalt mixture. In the dry method, the crumb rubber is first mixed with the aggregate and then sprayed into the asphalt and mixed to prepare a rubberized asphalt mixture [13,14]. In the wet method, crumb rubber is actually used as a modifier of asphalt, while crumb rubber is considered as part of the fine aggregate in the dry method [15]. Relevant literature has demonstrated that the wet process can significantly improve the viscosity of base asphalt [16], high-temperature performance [17], fatigue resistance [18], and low-temperature performance [19] of an asphalt mixture. In the dry process, the poor interaction between crumb rubber and asphalt makes pavement disease appear prematurely, which limits its application to a certain extent [15]. The most common technique used in rubber asphalt road construction is the wet process. The performance of crumb-rubber-modified asphalt is closely related to the performance of an asphalt mixture prepared with a wet process. Therefore, researchers have carried out extensive research on rubber-modified asphalt. Zhu et al. [20] reported that a higher rubber content means a higher softening point, ductility, elastic recovery, and lower penetration of crumb-rubber-modified asphalt. Further, using a dynamic shear rheometer and bending beam rheometer, it was found that the crumb-rubber-modified asphalt with a higher rubber content has higher high-temperature rutting resistance and low-temperature cracking resistance. Amir et al. [21] investigated the rutting resistance, fatigue properties, and rheological properties of nano-clay and rubber-composite-modified asphalt. The results showed that adding nano-clay to rubber asphalt can improve the rutting resistance and the temperature sensitivity of rubber asphalt. Additionally, nano-clay can retard the aging of asphalt and further improve the fatigue performance of asphalt.

As a by-product of the steel-making process, steel slag, like scrap tires, is also a serious threat to the ecological environment [22,23]. To address the above problems, researchers have achieved good research results using treated steel slag as road engineering materials and have applied these materials in practical engineering, especially in asphalt pavement [24–26]. Wu et al. [27] replaced 4.75–9.5 mm and 9.5–13 mm aggregates in SMA-13 with steel slag and evaluated the mixture performance. Their study found that taking steel slag as an aggregate could enhance the high-temperature and low-temperature performance of an SMA-13 mixture compared to basalt. Chen et al. [28] prepared an asphalt mixture with steel slag powder filler and characterized its road performance. They found that an asphalt mixture with steel slag powder filler rather than limestone filler showed greater water stability, high-temperature deformation resistance, and low-temperature crack resistance. The researchers also found that steel powder as a filler could improve the anti-rutting performance of asphalt mortar, while the crack resistance of asphalt mastic was slightly decreased [29,30]. However, Li et al. [31] found that asphalt mastic with steel slag powder had better low-temperature performance than asphalt mastic with limestone powder in cold regions. In summary, steel slag as a filler can significantly enhance the stiffness of asphalt, thereby improving the high-temperature deformation resistance of asphalt, but there is still controversy about the research on low-temperature performance. In addition, the performance and modification mechanism of steel slag powder and rubber-powder-composite-modified asphalt deserve further investigation.

In this paper, combined with the excellent elasticity and fatigue resistance of WTR and the outstanding stiffness of SSP, asphalt modified with steel slag powder and waste tire rubber compound was prepared. The physical properties of the asphalt with WTR and SSP compound, including the penetration, softening point, and viscosity, were investigated. Furthermore, the rutting resistance, fatigue performance, crack resistance, and mixing mechanism of asphalt modified with SSP and WTR were evaluated with a dynamic shear rheometer (DSR), bending beam rheometer (BBR), and Fourier transform infrared

spectrometer (FTIR). The results can provide a theoretical basis for the comprehensive utilization of waste tire rubber and steel slag.

2. Experimental Plan

2.1. Materials

The base asphalt with a 60/80 penetration grade was selected in this research, and the properties are displayed in Table 1.

Table 1. The properties of base asphalt.

Properties	Values	Requirements
Penetration (25 °C)	67.9	60–80
Softening point	47.8	≥46
Ductility 5 cm/min	183	≥100
Viscosity (60 °C)	230.5	≥100

The waste tire rubber powder (30 mesh) created by crushing waste tires was obtained. The density and main components of the waste tire rubber powder are shown in Table 2. The blast oxygen furnace slag stored for more than one year was obtained from Hubei Wuhan Iron and Steel Group Echeng Iron and Steel Co., Ltd. The steel slag powder was produced by grinding steel slag with a planetary ball mill and passing through a 0.075 mm sieve. The $d(0.1)$, $d(0.5)$, and $d(0.9)$ particle size distribution of steel slag powder were obtained by laser particle size analyzer to be 0.949 μm , 10.272 μm , and 44.181 μm , respectively. Meanwhile, the content of free CaO in steel slag was 1.83%, determined by ethylene glycol-EDTA chemical titration. The chemical composition of the steel slag powder determined by X-ray fluorescence is shown in Table 3. Macro appearances of waste tire rubber powder and steel slag powder are displayed in Figure 1. The laser particle size analysis results of the two fillers are shown in Figure 2.

Table 2. The technical parameters of waste tire rubber powder.

Parameters	Density (g/cm^3)	Moisture Content (%)	Metal Content (%)	Fiber Content (%)	Carbon Black Content (%)
Value	1.13	0.58	0.024	0.71	35

Table 3. The chemical composition of steel slag powder.

Compound	CaO	Fe ₂ O ₃	SiO ₂	MgO	Mn ₃ O ₄	Al ₂ O ₃	P ₂ O ₅	Others	LOI
Content (%)	39.83	24.03	15.36	8.53	4.56	3.12	1.88	2.35	0.34



Figure 1. Macro appearances of steel slag powder and waste tire rubber. (a) Waste tire rubber powder. (b) Steel slag powder.

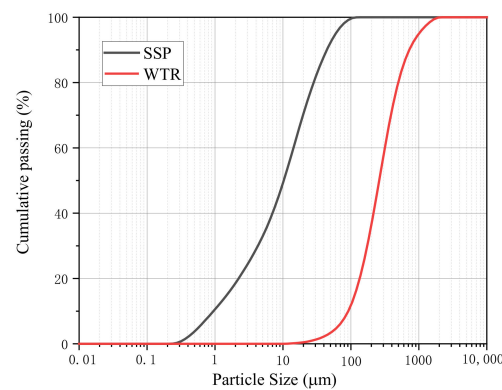


Figure 2. Particle size distribution of the SSP and WTR.

2.2. Methodology

2.2.1. Preparation of Asphalt Modified with Steel Slag Powder and Waste Tire Rubber Compound

Base asphalt was first heated at 135 °C for 1 h to make the asphalt flow. Then, a certain amount of waste tire rubber powder and steel slag powder was added to the asphalt and pre-stirred with a glass rod for 5 min. In this way, the modifier can be dispersed more evenly. Then, it was put into a high-speed shearing machine for 1 h at 4000 rpm and 180 °C. The same process was carried out for base asphalt. The preparation process is shown in Figure 3. The weight ratios of modifier and asphalt are shown in Table 4.

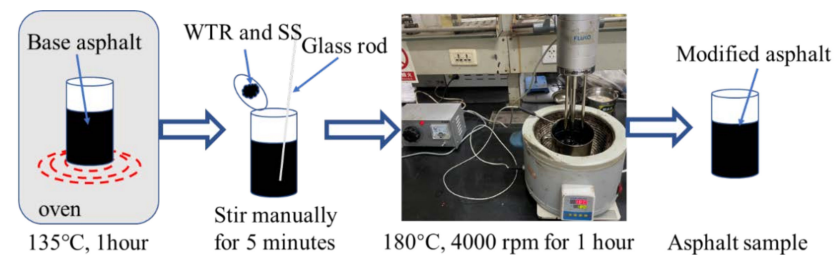


Figure 3. Preparation process of modified asphalt.

Table 4. The weight ratio of asphalt and modifier in modified asphalt.

Asphalt Samples	Asphalt	WTR	Steel Slag (SS)
Base asphalt	100	0	0
10%CR MA	100	10	0
8%CR + 2%SS MA	100	8	2
6%CR + 4%SS MA	100	6	4
4%CR + 6%SS MA	100	4	6
2%CR + 8%SS MA	100	2	8
10%SS MA	100	0	10

2.2.2. Physical Properties Tests

The penetration, softening point, and viscosity of base asphalt and asphalt modified with steel slag powder and waste tire rubber compound were performed based on JTG E20-2011 (T0604, T0606, and T0625) specifications, respectively. Penetration test temperature was 25 °C. The viscosity test temperature was 90 °C, 105 °C, 120 °C, 135 °C, and 150 °C, respectively. For each asphalt sample, three parallel samples were performed.

2.2.3. High-Temperature Rheological Properties Tests

The high-temperature rheological properties of asphalt are characterized by DSR tests [32]. The high-temperature property of asphalt samples was tested using a DSR

instrument (Anton Paar-101). The test temperature range was 30~80 °C, and the frequency was 10 rad/s.

The recovery rate R and non-recoverable creep compliance J_{nr} of asphalt samples were detected using a Multiple Stress Creep Recovery Test (MSCR). Asphalt samples were treated by short-term aging in a rolling film oven (RTFO) before MSCR test. In this research, the MSCR test was carried out for 20 cycles. All asphalt samples were tested for 10 creep recovery cycles at 0.1 kPa and 3.2 kPa, respectively. The creep time was 1 s, and the recovery time was 9 s in a single cycle. The test was conducted at 58 °C, and the calculation equation of R , J_{nr} , and $J_{nr-diff}$ are as follows [33,34]:

$$R = \frac{1}{10} \left\{ \sum_1^{10} \left(\frac{\varepsilon_r}{\varepsilon_{PeakStrain}} \times 100\% \right) \right\} \quad (1)$$

$$J_{nr-0.1} \left(\frac{1}{kPa} \right) = \frac{1}{10} \left\{ \sum_1^{10} \left(\frac{\varepsilon_{non-recoverable}}{0.1} \times 100\% \right) \right\} \quad (2)$$

$$J_{nr-3.2} \left(\frac{1}{kPa} \right) = \frac{1}{10} \left\{ \sum_1^{10} \left(\frac{\varepsilon_{non-recoverable}}{3.2} \times 100\% \right) \right\} \quad (3)$$

$$J_{nr-diff} = \frac{J_{nr(3.2kPa)} - J_{nr(0.1kPa)}}{J_{nr(0.1kPa)}} \quad (4)$$

where R is creep recovery rate; ε_r and $\varepsilon_{non-recoverable}$ were recoverable strain and non-recoverable strain in a single cycle, respectively; $\varepsilon_{Peakstrain}$ is the difference between the strain at the end of loading and the initial strain of loading in a single cycle; $J_{nr-0.1}$ and $J_{nr-3.2}$ are non-recoverable creep compliance of asphalt under stresses of 0.1 kPa and 3.2 kPa, respectively; and $J_{nr-diff}$ is stress sensitivity parameter.

2.2.4. Fatigue Performance Tests

The linear amplitude sweep (LAS) test evaluates the fatigue performance of asphalt at medium temperatures using DSR [35,36]. The rheological parameters in the failure process were obtained by applying linear strain to the asphalt, and the fatigue life of the asphalt was predicted by the viscoelastic continuum damage model. In this research, asphalt samples were subjected to RTFOT before asphalt fatigue testing with DSR according to AASHTO TP-101. First, the sample was subjected to a frequency sweep at 25 °C, and the frequency sweep range was 0.1~30 Hz. Then, linear amplitude sweep was conducted at 25 °C, which adopts the loading mode of strain control, a scanning time of 310 s, and a frequency of 10 Hz. The loading amplitude increased linearly from 0.1% to 30%. Fatigue life can be obtained by Equation (5) [35].

$$Nf = A \cdot (\gamma_{max})^B \quad (5)$$

where Nf is the failure life, γ_{max} is the maximum expected strain, and A and B are the model constants.

The characteristic parameter α of the undamaged material is determined by frequency sweep test, by which parameter B in the fatigue equation was calculated. The method for determining parameter α is as follows.

The storage modulus G' is obtained by complex modulus G^* and phase angle δ , and its calculation formula is as shown in Formula (6).

$$G'(\omega) = |G^*|(\omega) \times \cos \delta(\omega) \quad (6)$$

where ω is the frequency. We can take $\log \omega$ as the abscissa and $\log G'(\omega)$ as the ordinate and draw and fit an optimal straight line: $\log G'(\omega) = m(\log \omega) + b$. Then, parameter α and B can be obtained by Formulas (7) and (8) [35].

$$\alpha = 1 + \frac{1}{m} \quad (7)$$

$$B = 2\alpha \quad (8)$$

According to the test data of linear amplitude sweep, the calculation formula of damage accumulation of asphalt is Formula (9) [35].

$$D(t) = \sum \left[\pi(\gamma_i)^2 (C_{i-1} - C_i) \right]^{\frac{\alpha}{1+\alpha}} (t_i - t_{i-1})^{\frac{1}{1+\alpha}} \quad (9)$$

where $D(t)$ is the damage accumulation at time t , γ_i is the shear strain and C_i equals $\left(\frac{G^*(t)}{G^*(initial)}\right)$, G^* is complex modulus, and α is the characteristic parameter of the undamaged material. $D(t)$ and C can be obtained by performing linear regression. The A value is also obtained according to Equations (10)~(13) [35]:

$$\text{Log}(C_0 - C(t)) = \text{Log}C_1 + C_2 \text{Log}[D(t)] \quad (10)$$

$$A = \frac{f \cdot (D_f)^k}{k(\pi C_1 C_2)^\alpha} \quad (11)$$

$$D_f = \left(\frac{C_0 - C_{PeakStress}}{C_1} \right)^{1/C_2} \quad (12)$$

$$k = 1 + \alpha(1 - C_2) \quad (13)$$

where C_0 represents initial value of integrity parameter, f represents frequency, and C_1 and C_2 are curve-fit coefficients.

2.2.5. Low-Temperature Performance Tests

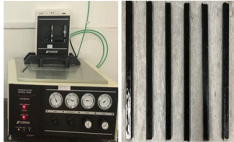
The stiffness modulus S and creep rate m of asphalt tested by BBR under constant loading are used to evaluate the low-temperature performance of asphalt [11,20]. Asphalt sample size was $127 \times 6.35 \times 12.7$ mm. The test temperatures were set to -12 °C, -18 °C, and -24 °C, respectively.

2.2.6. FTIR Tests

In this paper, Nicolet 6700 infrared spectrometer produced by Thermo Fisher Scientific Company was used to characterize the types of functional groups in asphalt and asphalt modified with WTR and SSP. The test wave number range is $400\sim 4000$ cm^{-1} .

The relevant test instruments and samples are shown in Table 5.

Table 5. Information on relevant tests.

Performance	Instruments and Samples Figure	Conducted Test
High temperature		Temperature-sweep tests
Medium temperature		MSCR tests
Low temperature		LAS tests
Modified mechanism		BBR tests
		FTIR tests

3. Results and Discussion

3.1. Physical Properties

The penetration of asphalt can reflect the consistency of asphalt. The smaller the penetration of asphalt, the harder the asphalt and the greater the consistency. The softening point of asphalt can characterize the viscosity and high-temperature stability. Asphalt with a higher softening point has better high-temperature stability. Generally, with the same material, the penetration shows an opposing trend to the softening point, as displayed in Figure 4. Clearly, the penetration of asphalt can be reduced, and the softening point of asphalt can be raised by adding WTR or SSP. With the same content of WTR and SSP, the penetration and softening point of WTR-modified asphalt changed more prominently, which may be attributed to the three-dimensional network structure formed by WTR, which limits the flow of asphalt [20,37]. This phenomenon occurs in SSP-modified asphalt because the porous structure of steel slag absorbs the components of asphalt, which leads to a decrease in free asphalt and an increase in structural asphalt [30]. When the total content of WTR and SSP is constant, the softening point of asphalt modified with WTR and SSP gradually decreases, and the penetration is contrary to the decrease in the ratio of WTR to SSP.

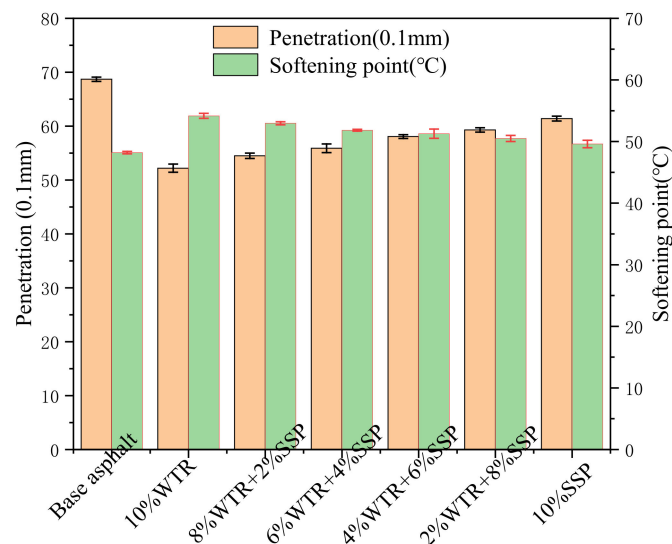


Figure 4. The penetration and softening point test results.

The Arrhenius Equation (14) is widely used in describing the viscosity-temperature relationship of asphalt [33]:

$$\eta = A \cdot e^{E_{\eta}/RT} \quad (14)$$

$$\ln \eta = \ln A + \frac{E_{\eta}}{R} \times \frac{1}{T} \quad (15)$$

where η is the viscosity of asphalt binders; A is the regression coefficient; R is the universal gas constant, $R = 8.314 \text{ J}/(\text{mol} \cdot \text{K})$; and T represents absolute temperature. E_{η} represents the flow activation energy; the material with a smaller E_{η} flows easier and exhibits higher temperature sensitivity.

Figure 5 shows the viscosity-temperature relationship of asphalt and a straight line fitted using the Arrhenius Equation (15). The viscosity of the base asphalt is the lowest at the same temperature, and the addition of WTR or SSP can visibly augment the viscosity of base asphalt. In addition, with the same content of WTR and SSP, the WTR-modified asphalt has a higher viscosity than that of SSP-modified asphalt. When the total content of WTR and SSP remains unchanged, with the decrease in the ratio of WTR to SSP, the viscosity of asphalt modified with WTR and SSP gradually decreases. The relevant parameters obtained by fitting the viscosity-temperature test data with the Arrhenius equation are shown in

Table 6. The fitting accuracy R^2 is above 0.99, which means that the relationship between the viscosity and temperature of asphalt can be described by the Arrhenius equation well. It is obvious that adding WTR or SSP can enhance the flow activation energy E_η of asphalt. A larger E_η indicates that the asphalt is less likely to flow and thus has lower temperature sensitivity [38]. It also further means that the SSP-modified asphalt has a higher temperature sensitivity than WTR-modified asphalt. The viscosity test results are in accord with the results of softening point test.

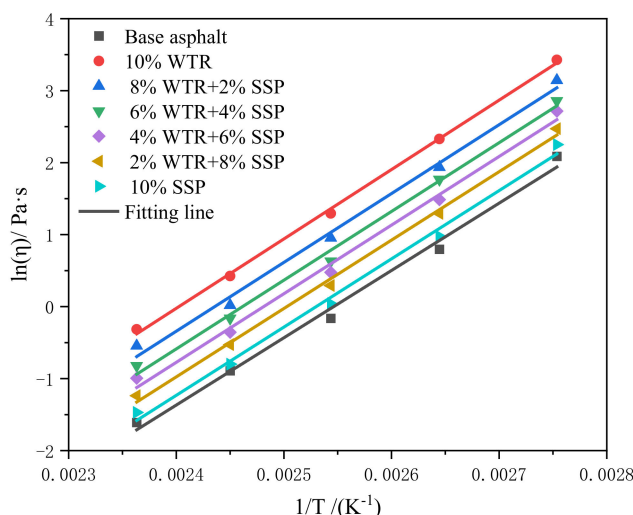


Figure 5. The viscosity-temperature relationships.

Table 6. Relevant parameters of Arrhenius equation fitting.

Samples	Fitting Line	R^2	Slope (E_η/R)	E_η (kJ/mol)
Base asphalt	$y = 9349.9x - 23.8$	0.99215	9349.9	77.73
10% WTR	$y = 9640.1x - 23.2$	0.99874	9640.1	80.15
8%WTR + 2%SSP	$y = 9563.1x - 23.3$	0.99364	9563.1	79.51
6%WTR + 4%SSP	$y = 9550.1x - 23.5$	0.99487	9550.1	79.40
4%WTR + 6%SSP	$y = 9533.4x - 23.7$	0.99384	9533.4	79.26
2%WTR + 8%SSP	$y = 9501.4x - 23.8$	0.99677	9501.4	78.99
10%SSP	$y = 9480.7x - 24.0$	0.99404	9480.7	78.82

3.2. High-Temperature Rheological Properties

The mechanical behaviors of asphalt are affected by time and temperature [38]. The DSR test was employed to obtain two important parameters (complex modulus G^* and phase angle δ). G^* is a measure of the total resistance of the material during repeated shear deformation, and δ is the time lag between the applied stress and the resulting strain. The stronger the elasticity of the material, the closer δ is to 0.

The curve of G^* and δ of asphalt samples with different modifier dosages is illustrated in Figure 6. In Figure 6a, the G^* of all samples decreases with the rise in temperature. That is, as temperature increases, the asphalt gradually changes from a solid state to a viscous flow state. Additionally, the G^* -modified asphalt with WTR or SSP is higher than that of base asphalt at 30~80 °C. However, the G^* of SSP-modified asphalt and WTR-modified asphalt cross at about 45 °C. That is, the SSP-modified asphalt has a higher G^* than that of WTR-modified asphalt at 30~45 °C, while the pattern is reversed at 45~80 °C. In Figure 6b, the δ of the base asphalt and the SSP-modified asphalt gradually approaches 90° with the rise in temperature. However, it was found that the δ of the WTR-modified asphalt appeared at a phase angle plateau at 30~50 °C, and the phase angle platform gradually disappeared with the decrease in the ratio of WTR to steel slag. This can be attributed to the three-dimensional network structure formed by WTR, which limits the flow of asphalt [39].

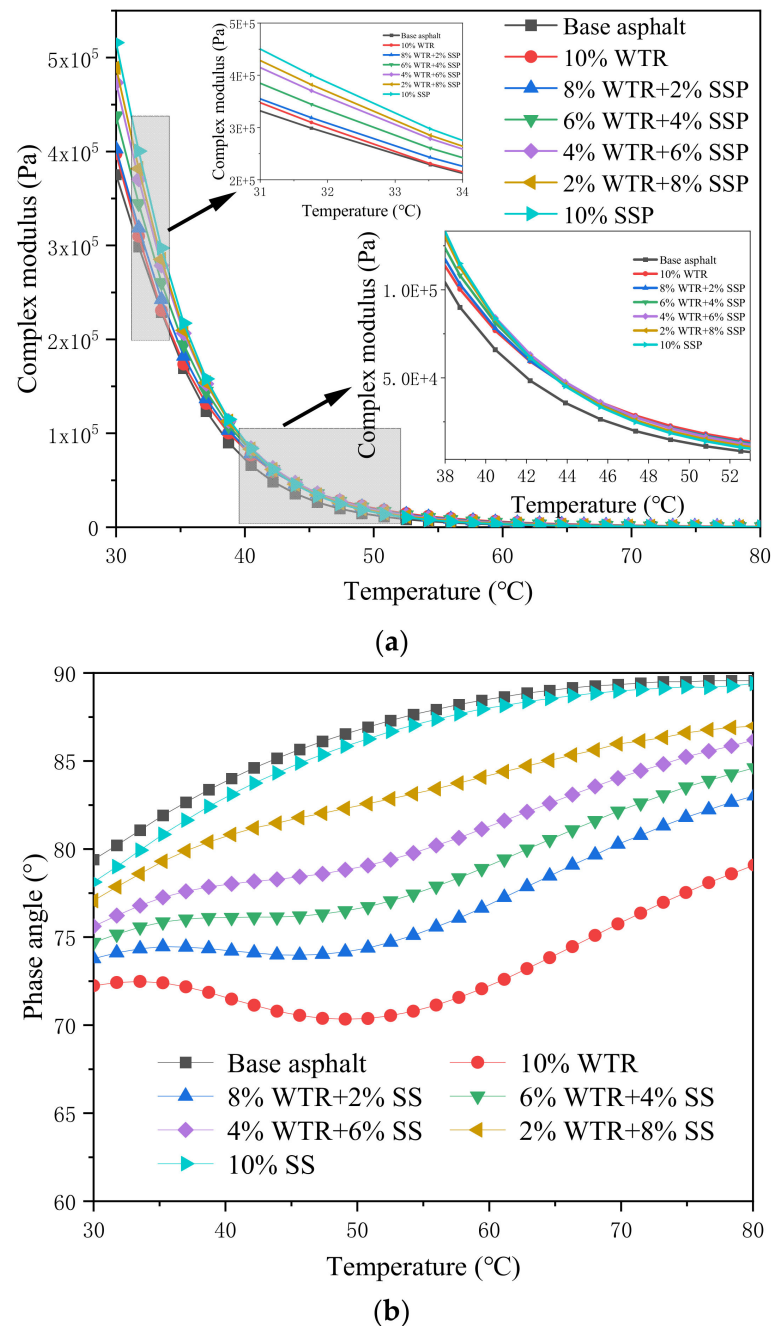


Figure 6. The results of temperature sweep: (a) complex modulus; (b) phase angle.

Rutting is a serious disease type of asphalt pavement, and the rutting resistance of asphalt is one of the important factors affecting the performance of asphalt pavement. The American Strategic Highway Research Program (SHRP) proposes to use the rutting factor $G^*/\sin \delta$ to characterize the rutting resistance of asphalt. The larger the $G^*/\sin \delta$, the better the high-temperature performance. In Figure 7, the rutting factor of all samples decreased with the rise in temperature. The $G^*/\sin \delta$ of base asphalt is the smallest, indicating it has the worst rutting resistance. However, the $G^*/\sin \delta$ of SSP-modified asphalt and WTR-modified asphalt cross at about 42 °C. Thus, the anti-rutting performance of SSP-modified asphalt is better than that of WTR-modified asphalt at 30~42 °C, while the pattern is reversed at 42~80 °C. The high-temperature rutting resistance of the asphalt WTR and SSP compound is between WTR-modified asphalt and SSP-modified asphalt.

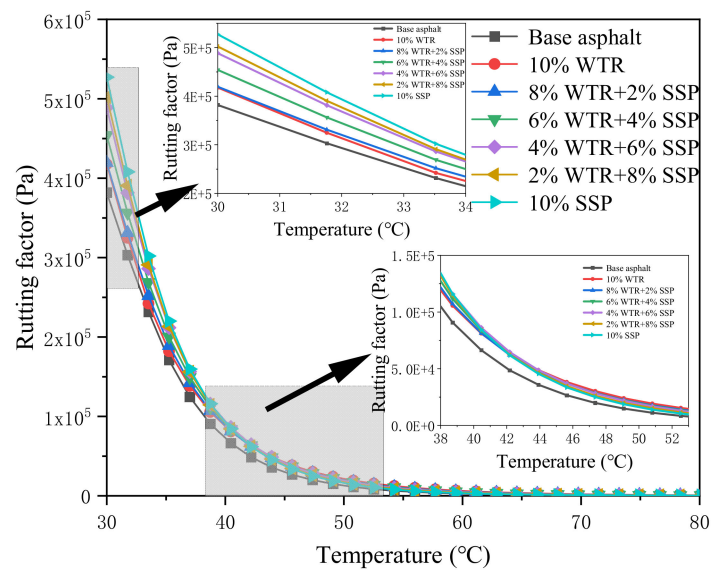


Figure 7. Relationship curve between rutting factor and temperature.

The MSCR test is recognized for characterizing the permanent deformation resistance of asphalt [40]. The relationship between the cumulative strain and time under different stress levels is described in Figure 8. The accumulative strain of WTR-modified asphalt is less than that of SSP-modified asphalt, which is less than that of base asphalt. Moreover, when the total content of WTR and SSP is constant, the accumulative strain of the asphalt modified with WTR and SSP compound declines with the increase in the ratio of WTR and SSP. The relevant indicators (R , J_{nr} , and $J_{nr-diff}$) from the MSCR test are shown in Table 7. Under different stress levels (0.1 and 3.2 kPa), base asphalt has the smallest R and the largest J_{nr} . Incorporating WTR or SSP into the base asphalt can enhance the R and reduce the J_{nr} . Under the same content of WTR and SSP, the creep recovery rate of WTR-modified asphalt is higher than that of SSP-modified asphalt. When the total content of WTR and SSP is constant, the R of the asphalt modified with WTR and SSP compound increases with the rise in the ratio of WTR and SSP. In addition, the stress sensitivity index $J_{nr-diff}$ of 10% WTR-modified asphalt is the highest, reaching 52.78%. The AASHTO MP19-10 specification requires that the stress sensitivity index $J_{nr-diff}$ does not exceed 75% [36]. Therefore, the stress sensitivity of all asphalt samples meets the specification requirements.

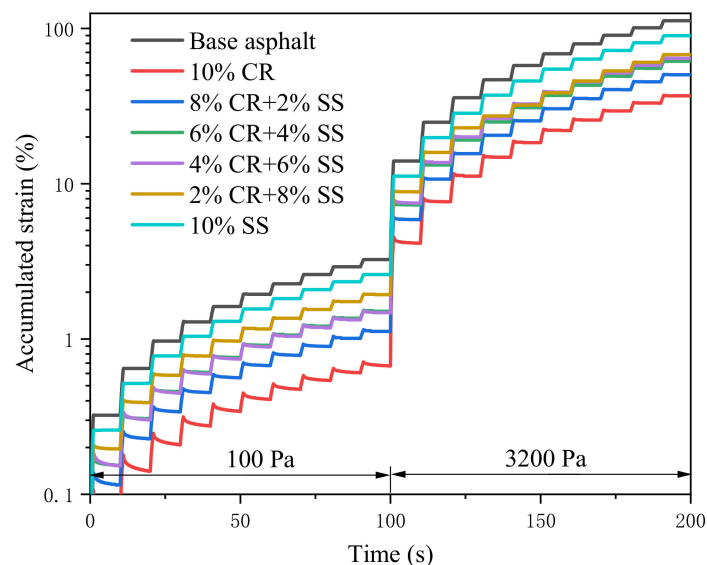


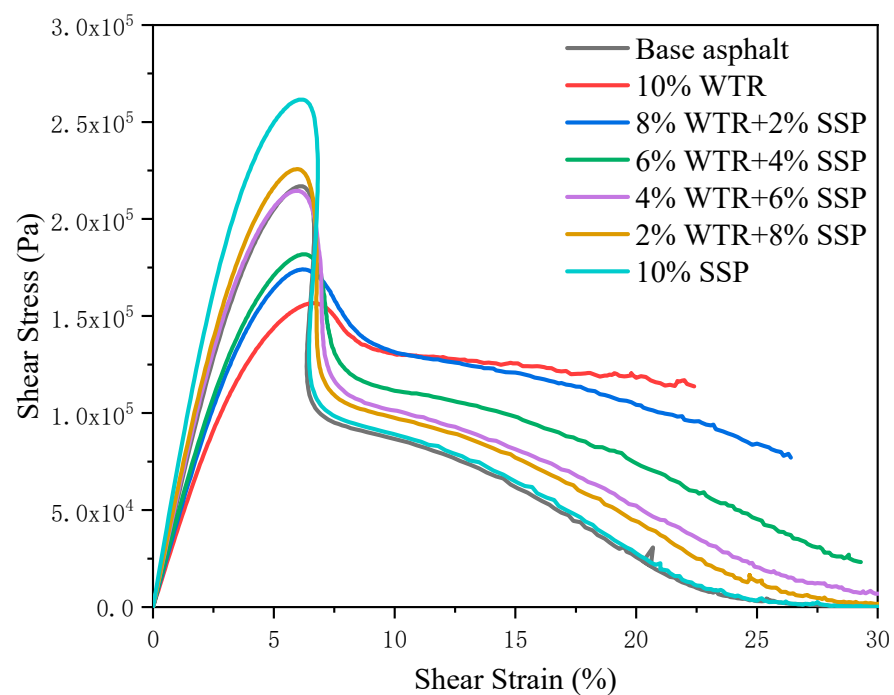
Figure 8. The accumulated strain-time curve of MSCR.

Table 7. The relevant indicators of MSCR test results.

Samples	R-100	R-3200	J_{nr-100}	$J_{nr-3200}$	$J_{nr-diff}$
Base asphalt	3.33	0.43	3.23	3.35	3.72
10% WTR	35.45	10.46	0.72	1.10	52.78
8% WTR + 2%SSP	18.71	3.98	1.15	1.51	31.30
6% WTR + 4%SSP	10.59	2.07	1.52	1.84	21.05
4% WTR + 6%SSP	6.47	1.24	1.70	1.94	14.12
2% WTR + 8%SSP	4.91	0.70	1.96	2.20	12.24
10%SSP	3.54	0.52	2.59	2.69	3.86

3.3. Fatigue Properties

Figure 9 presents the stress-strain curve of asphalt at 25 °C in the LAS test. Obviously, the base asphalt and SSP-modified asphalt yield with the increase in strain, and the WTR-modified asphalt does not yield. The peak stress is an indicator that characterizes the hardness of the material in the LAS. The greater the peak stress, the harder the material. SSP-modified asphalt has the largest peak stress at 25 °C, and the peak stress of WTR-modified asphalt is the lowest. Thus, the hardness of SSP-modified asphalt is greater than that of WTR-modified asphalt at 25 °C. However, the high peak stress in the LAS test does not necessarily mean that the material has good fatigue properties [12].

**Figure 9.** The stress-strain curve of asphalt samples of LAS test.

According to the test results of frequency sweep, amplitude sweep, and viscoelastic continuous damage theory, the fatigue life of asphalt was further predicted by parameters A and B. When parameter B value is constant, the high A value can enhance the fatigue life of asphalt, and the high B value decreases the fatigue life of the asphalt. The relevant fatigue performance parameters from the LAS test are displayed in Table 8. Apparently, the fatigue life of base asphalt is the lowest. Incorporating WTR or SSP in asphalt can enhance the fatigue life. In addition, the incorporation of WTR has a more prominently modification effect on the fatigue life. Compared with base asphalt, asphalt modified with 10% WTR and 10% SSP increases the fatigue life of asphalt by 70.2% and 20.3% at the 2.5 strain level and 10.2% and 5.3% at the 5% strain level, respectively. When the total content of WTR and SSP

is constant, as the ratio of WTR and SSP decreases, the fatigue life of composite-modified asphalt shows a decreasing trend.

Table 8. The fatigue parameters from LAS test.

Asphalt	LAS Parameters (25 °C)			
	A	B	Nf (2.5%)	Nf (5%)
Base asphalt	7.986×10^6	−3.868	230,726	15,802
10% WTR	2.064×10^7	−4.321	393,741	19,700
8%WTR + 2%SSP	1.738×10^7	−4.230	360,382	19,205
6%WTR + 4%SSP	1.482×10^7	−4.160	327,656	18,329
4%WTR + 6%SSP	1.382×10^7	−4.129	314,350	17,966
2%WTR + 8%SSP	1.211×10^7	−4.051	295,862	17,849
10% SSP	9.266×10^6	−3.924	254,317	16,755

3.4. Low-Temperature Rheological Properties

BBR tests were undertaken to determine the creep stiffness S and creep stiffness change rate m of the asphalt at -12 , -18 , and -24 °C, as illustrated in Figure 10. The larger the S value, the harder the asphalt. A low m value indicates that the asphalt has a low deformation and stress-dissipation capacity. Generally, a lower S value and a higher m value mean that asphalt has better low-temperature performance [41]. In Figure 10a,b, for all asphalt samples, the S value increases while the m value declines as the temperature decreases. That is, as the temperature decreases, the asphalt gradually becomes hard, showing brittleness, and the low-temperature performance decreases. WTR-modified asphalt can obviously decrease the S value, enlarge the m value, and enhance the low-temperature performance. The S value and m value of base asphalt and 10% SSP-modified asphalt show almost no difference. Therefore, SSP has little effect on the low-temperature performance of asphalt. SHRP specifications require that the maximum S value at 60 s is lower than 300 MPa, and the m values need to be larger than 0.3 [42]. It can be seen that asphalt modified with 10% WTR can meet the specification requirements at -12 °C, while 10% SSP-modified asphalt slightly exceeds the specification requirements. Moreover, all asphalt samples at -18 and -24 °C did not meet the specification requirements at low temperatures.

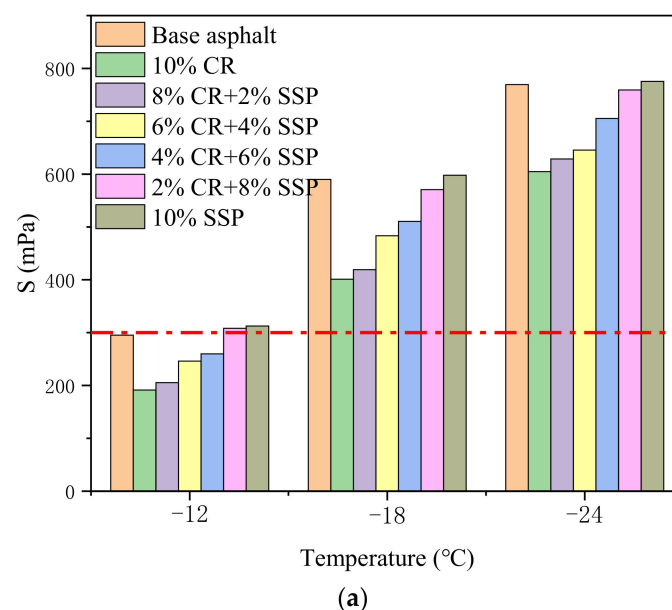


Figure 10. Cont.

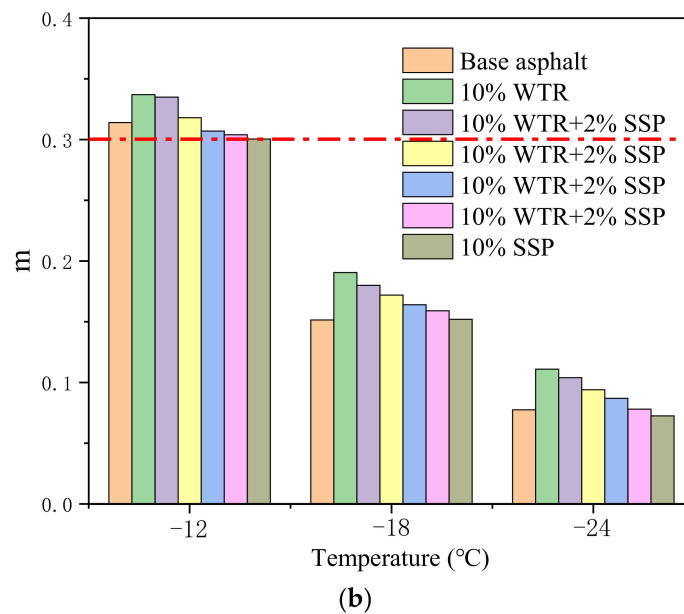


Figure 10. The result of low temperatures in the BBR test. (a) Creep stiffness; (b) creep rate.

3.5. FTIR Results

Infrared spectroscopy is an important method for analyzing the structure of organic compounds [43]. Therefore, the blending mechanism of asphalt modified with WTR and SSP was explored by the variety of functional groups in the infrared spectrum. The infrared spectra of asphalt are displayed in Figure 11. In Figure 11, all asphalt samples have peaks at 2924, 2853, 1600, 1458, and 1376 cm^{-1} , of which 2924 and 2850 cm^{-1} are the stretching vibration of C-H in aliphatic hydrocarbons, 1458 cm^{-1} and 1376 cm^{-1} are the C-H bending vibration in methylene and methyl, and 1600 cm^{-1} is the stretching vibration of C=C in aromatics3 [41,44,45]. Compared to base asphalt, there are no new peaks in the two kinds of modified asphalt. Thus, the modification of asphalt by two modifiers is mainly a physical process.

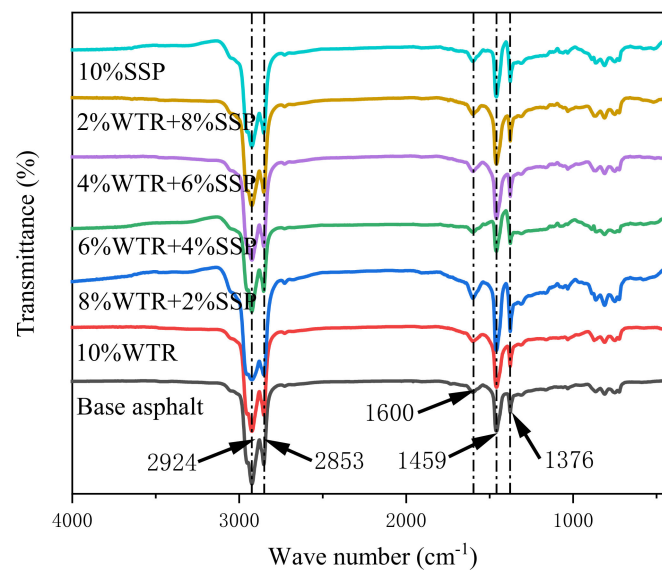


Figure 11. The infrared spectrum of all asphalt samples.

4. Conclusions

In this paper, asphalt modified with SSP and WTR was prepared. The physical properties, high-temperature performance, low-temperature performance, fatigue resistance, and

blending mechanism of asphalt modified with WTR and SSP were discussed through an array of characterizations. The conclusions are as follows.

- Both WTR and SSP can reduce the penetration and improve the softening point and viscosity of asphalt. WTR-modified asphalt had a higher viscosity, fatigue life, and creep stiffness change rate than steel-slag-powder-modified asphalt with the same content, indicating its superior road performance.
- The complex modulus-temperature curves of WTR-modified asphalt and SSP-modified asphalt cross at around 45 °C. When the temperature is higher than 45 °C, compound-modified asphalt has a larger complex modulus than that of SSP-modified asphalt, endowing it with better rutting resistance. This is attributed to the three-dimensional network structure of WTR that hinders the transformation of WTR-modified asphalt from the viscoelastic state to the viscous flow state.
- The physical properties, fatigue performance, and low-temperature performance of asphalt modified with SSP and WTR decrease with the decrease in the ratio of WTR and SSP with the same total content of WTR and SSP. At lower temperatures, the elasticity of the compound-modified asphalt is mainly provided by SSP, while WTR dominates its rutting factor at higher temperatures.
- Compared with base asphalt, SSP-modified asphalt and WTR-modified asphalt have lower temperature sensitivity and higher stress sensitivity. The temperature sensitivity of WTR-modified asphalt is lower than that of SSP-modified asphalt, while the stress sensitivity is higher than that of SSP-modified asphalt. Infrared spectrum results verified that the preparation of WTR- and SSP-modified asphalt is a physical blending process.

The above conclusions have certified that the compound-modified asphalt with WTR and SSP combines the advantages of WTR and SSP, which not only improves the high-temperature rutting resistance, medium-temperature fatigue properties, and low-temperature crack resistance of SSP-modified asphalt but also improves the temperature sensitivity and stress sensitivity of WTR-modified asphalt. These results are helpful for promoting the utilization of WTR and SSP. Further studies are necessary to explore the effect of steel-slag- and rubber-compound-modified asphalt on the performance of an asphalt mixture.

Author Contributions: Z.W.: Conceptualization, Methodology, Investigation, Data Curation, and Writing—Original Draft. Z.Z.: Conceptualization, Project Administration, Review and Editing, and Supervision. C.Y., S.C. and Y.Z.: Review and Editing. X.Y.: Conceptualization, Methodology. All authors have read and agreed to the published version of the manuscript.

Funding: This research was sponsored by the National Key R&D Program of China (no. 2018YFB-1600200), the Key R&D Program of Guangxi Province (no. 2021AB26023), the Key R&D Program of Hubei Province (no. 2020BCB064), and the Hebei Provincial Communication Department project (no. YC-201926).

Institutional Review Board Statement: Not applicable.

Informed Consent Statement: Not applicable.

Data Availability Statement: The data presented in this study were available on request from the corresponding author.

Conflicts of Interest: The authors declare no conflict of interest.

References

1. Selsal, Z.; Karakas, A.S.; Sayin, B. Effect of pavement thickness on stress distribution in asphalt pavements under traffic loads. *Case Stud. Constr. Mater.* **2022**, *16*, e01107. [[CrossRef](#)]
2. Li, N.; Jiang, Q.; Wang, F.; Cui, P.; Xie, J.; Li, J.; Wu, S.; Barbieri, D.M. Comparative Assessment of Asphalt Volatile Organic Compounds Emission from field to laboratory. *J. Clean. Prod.* **2021**, *278*, 123479. [[CrossRef](#)]
3. Sahebzamani, H.; Alavi, M.Z.; Farzaneh, O. Evaluating effectiveness of polymerized pellets mix additives on improving asphalt mix properties. *Constr. Build. Mater.* **2018**, *187*, 160–167. [[CrossRef](#)]

4. Duarte, G.M.; Faxina, A.L. Asphalt concrete mixtures modified with polymeric waste by the wet and dry processes: A literature review. *Constr. Build. Mater.* **2021**, *312*, 125408. [[CrossRef](#)]
5. Viscione, N.; Lo Presti, D.; Veropalumbo, R.; Oretto, C.; Biancardo, S.A.; Russo, F. Performance-based characterization of recycled polymer modified asphalt mixture. *Constr. Build. Mater.* **2021**, *310*, 125243. [[CrossRef](#)]
6. Tang, N.; Huang, W.; Hao, G. Effect of aging on morphology, rheology, and chemical properties of highly polymer modified asphalt binders. *Constr. Build. Mater.* **2021**, *281*, 122595. [[CrossRef](#)]
7. Zhang, H.; Xu, G.; Chen, X.; Wang, R.; Shen, K. Effect of long-term laboratory aging on rheological properties and cracking resistance of polymer-modified asphalt binders at intermediate and low temperature range. *Constr. Build. Mater.* **2019**, *226*, 767–777. [[CrossRef](#)]
8. Dwivedi, C.; Manjare, S.; Rajan, S.K. Recycling of waste tire by pyrolysis to recover carbon black: Alternative & environment-friendly reinforcing filler for natural rubber compounds. *Compos. Part B Eng.* **2020**, *200*, 108346.
9. Al-Attar, A.A.; Hamada, H.M.; Tayeh, B.A.; Awoyera, P.O. Exploring engineering properties of waste tire rubber for construction applications—A review of recent advances. *Mater. Today Proc.* **2022**, *53*, A1–A17. [[CrossRef](#)]
10. Rodríguez-Fernández, I.; Tarpoudi Baheri, F.; Cavalli, M.C.; Poulikakos, L.D.; Bueno, M. Microstructure analysis and mechanical performance of crumb rubber modified asphalt concrete using the dry process. *Constr. Build. Mater.* **2020**, *259*, 119662. [[CrossRef](#)]
11. Lv, S.; Ma, W.; Zhao, Z.; Guo, S. Improvement on the high-temperature stability and anti-aging performance of the rubberized asphalt binder with the Lucobit additive. *Constr. Build. Mater.* **2021**, *299*, 124304. [[CrossRef](#)]
12. Yan, C.; Yuan, L.; Yu, X.; Ji, S.; Zhou, Z. Characterizing the fatigue resistance of multiple modified asphalts using time sweep test, LAS test and elastic recovery test. *Constr. Build. Mater.* **2022**, *322*, 125806. [[CrossRef](#)]
13. Alsaif, A.; Albidah, A.; Abadel, A.; Abbas, H.; Al-Salloum, Y. Development of metakaolin-based geopolymer rubberized concrete: Fresh and hardened properties. *Arch. Civ. Mech. Eng.* **2022**, *22*, 144. [[CrossRef](#)]
14. Bakheit, I.; Xiaoming, H. Modification of the dry method for mixing crumb rubber modifier with aggregate and asphalt based on the binder mix design. *Constr. Build. Mater.* **2019**, *220*, 278–284. [[CrossRef](#)]
15. Chavez, F.; Marcobal, J.; Gallego, J. Laboratory evaluation of the mechanical properties of asphalt mixtures with rubber incorporated by the wet, dry, and semi-wet process. *Constr. Build. Mater.* **2019**, *205*, 164–174. [[CrossRef](#)]
16. Li, P.; Jiang, X.; Ding, Z.; Zhao, J.; Shen, M. Analysis of viscosity and composition properties for crumb rubber modified asphalt. *Constr. Build. Mater.* **2018**, *169*, 638–647. [[CrossRef](#)]
17. Fontes, L.P.T.L.; Trichês, G.; Pais, J.C.; Pereira, P.A.A. Evaluating permanent deformation in asphalt rubber mixtures. *Constr. Build. Mater.* **2010**, *24*, 1193–1200. [[CrossRef](#)]
18. Picado-Santos, L.G.; Capitão, S.D.; Neves, J.M.C. Crumb rubber asphalt mixtures: A literature review. *Constr. Build. Mater.* **2020**, *247*, 118577. [[CrossRef](#)]
19. Razmi, A.; Mirsayar, M.M. Fracture resistance of asphalt concrete modified with crumb rubber at low temperatures. *Int. J. Pavement Res. Technol.* **2018**, *11*, 265–273. [[CrossRef](#)]
20. Zhu, Y.; Xu, G.; Ma, T.; Fan, J.; Li, S. Performances of rubber asphalt with middle/high content of waste tire crumb rubber. *Constr. Build. Mater.* **2022**, *335*, 127488. [[CrossRef](#)]
21. Amini, A.; Ziari, H.; Saadatjoo, S.A.; Hashemifar, N.S.; Goli, A. Rutting resistance, fatigue properties and temperature susceptibility of nano clay modified asphalt rubber binder. *Constr. Build. Mater.* **2021**, *267*, 120946. [[CrossRef](#)]
22. Cui, P.; Wu, S.; Xiao, Y.; Hu, R.; Yang, T. Environmental performance and functional analysis of chip seals with recycled basic oxygen furnace slag as aggregate. *J. Hazard. Mater.* **2021**, *405*, 124441. [[CrossRef](#)] [[PubMed](#)]
23. Li, J.; Yu, J.; Wu, S.; Xie, J. The Mechanical Resistance of Asphalt Mixture with Steel Slag to Deformation and Skid Degradation Based on Laboratory Accelerated Heavy Loading Test. *Materials* **2022**, *15*, 911. [[CrossRef](#)] [[PubMed](#)]
24. Gan, Y.; Li, C.; Ke, W.; Deng, Q.; Yu, T. Study on pavement performance of steel slag asphalt mixture based on surface treatment. *Case Stud. Constr. Mater.* **2022**, *16*, e01131. [[CrossRef](#)]
25. Li, L.; Ling, T.-C.; Pan, S.-Y. Environmental benefit assessment of steel slag utilization and carbonation: A systematic review. *Sci. Total Environ.* **2022**, *806*, 150280. [[CrossRef](#)]
26. Yang, C.; Wu, S.; Cui, P.; Amirkhanian, S.; Zhao, Z.; Wang, F.; Zhang, L.; Wei, M.; Zhou, X.; Xie, J. Performance characterization and enhancement mechanism of recycled asphalt mixtures involving high RAP content and steel slag. *J. Clean. Prod.* **2022**, *336*, 130484. [[CrossRef](#)]
27. Wu, S.; Xue, Y.; Ye, Q.; Chen, Y. Utilization of steel slag as aggregates for stone mastic asphalt (SMA) mixtures. *Build. Environ.* **2007**, *42*, 2580–2585. [[CrossRef](#)]
28. Chen, Z.; Leng, Z.; Jiao, Y.; Xu, F.; Lin, J.; Wang, H.; Cai, J.; Zhu, L.; Zhang, Y.; Feng, N.; et al. Innovative use of industrially produced steel slag powders in asphalt mixture to replace mineral fillers. *J. Clean. Prod.* **2022**, *344*, 131124. [[CrossRef](#)]
29. Li, C.; Chen, Z.; Wu, S.; Li, B.; Xie, J.; Xiao, Y. Effects of steel slag fillers on the rheological properties of asphalt mastic. *Constr. Build. Mater.* **2017**, *145*, 383–391. [[CrossRef](#)]
30. Tao, G.; Xiao, Y.; Yang, L.; Cui, P.; Kong, D.; Xue, Y. Characteristics of steel slag filler and its influence on rheological properties of asphalt mortar. *Constr. Build. Mater.* **2019**, *201*, 439–446. [[CrossRef](#)]
31. Li, Q.; Qiu, Y.; Rahman, A.; Ding, H. Application of steel slag powder to enhance the low-temperature fracture properties of asphalt mastic and its corresponding mechanism. *J. Clean. Prod.* **2018**, *184*, 21–31. [[CrossRef](#)]

32. Li, Y.; Feng, J.; Yang, F.; Wu, S.; Liu, Q.; Bai, T.; Liu, Z.; Li, C.; Gu, D.; Chen, A.; et al. Gradient aging behaviors of asphalt aged by ultraviolet lights with various intensities. *Constr. Build. Mater.* **2021**, *295*, 123618. [[CrossRef](#)]
33. Zhao, Z.; Wu, S.; Liu, Q.; Xie, J.; Yang, C.; Wang, F.; Wan, P. Recycling waste disposable medical masks in improving the performance of asphalt and asphalt mixtures. *Constr. Build. Mater.* **2022**, *337*, 127621. [[CrossRef](#)]
34. Zhang, L.; Xing, C.; Gao, F.; Li, T.-S.; Tan, Y.-Q. Using DSR and MSCR tests to characterize high temperature performance of different rubber modified asphalt. *Constr. Build. Mater.* **2016**, *127*, 466–474. [[CrossRef](#)]
35. Chen, H.; Bahia, H.U. Modelling effects of aging on asphalt binder fatigue using complex modulus and the LAS test. *Int. J. Fatigue* **2021**, *146*, 106150. [[CrossRef](#)]
36. Daryaei, D.; Habibpour, M.; Gulzar, S.; Underwood, B.S. Combined effect of waste polymer and rejuvenator on performance properties of reclaimed asphalt binder. *Constr. Build. Mater.* **2021**, *268*, 121059. [[CrossRef](#)]
37. Xu, G.; Kong, P.; Yu, Y.; Yang, J.; Zhu, M.; Chen, X. Rheological properties of rubber modified asphalt as function of waste tire rubber reclaiming degree. *J. Clean. Prod.* **2022**, *332*, 130113. [[CrossRef](#)]
38. Zhao, Z.; Wu, S.; Liu, Q.; Xie, J.; Yang, C.; Wan, P.; Guo, S.; Ma, W. Characteristics of calcareous sand filler and its influence on physical and rheological properties of asphalt mastic. *Constr. Build. Mater.* **2021**, *301*, 124112. [[CrossRef](#)]
39. Ma, J.; Sun, G.; Sun, D.; Zhang, Y.; Cannone Falchetto, A.; Lu, T.; Hu, M.; Yuan, Y. Rubber asphalt modified with waste cooking oil residue: Optimized preparation, rheological property, storage stability and aging characteristic. *Constr. Build. Mater.* **2020**, *258*, 120372. [[CrossRef](#)]
40. Gajewski, M.; Bańkowski, W.; Gajewska, B.; Sybilski, D.; Horodecka, R. Estimation of asphalt binders' resistance to permanent deformation with application of the MSCR and multiple shear creep long recovery (MSCLR) tests. *Constr. Build. Mater.* **2021**, *284*, 122808. [[CrossRef](#)]
41. Dong, Z.-J.; Zhou, T.; Luan, H.; Williams, R.C.; Wang, P.; Leng, Z. Composite modification mechanism of blended bio-asphalt combining styrene-butadiene-styrene with crumb rubber: A sustainable and environmental-friendly solution for wastes. *J. Clean. Prod.* **2019**, *214*, 593–605. [[CrossRef](#)]
42. Ren, H.; Qian, Z.; Huang, W.; Li, H.; Liu, Y. Low-temperature thermal cracking performance of waterborne epoxy asphalt emulsion mastic based on bending beam rheometer (BBR). *Constr. Build. Mater.* **2022**, *334*, 127461. [[CrossRef](#)]
43. Ding, H.; Hesp, S.A.M. Variable-temperature Fourier-transform infrared spectroscopy study of asphalt binders from the SHRP Materials Reference Library. *Fuel* **2021**, *298*, 120819. [[CrossRef](#)]
44. Leng, Z.; Padhan, R.K.; Sreram, A. Production of a sustainable paving material through chemical recycling of waste PET into crumb rubber modified asphalt. *J. Clean. Prod.* **2018**, *180*, 682–688. [[CrossRef](#)]
45. Alghrafy, Y.M.; Abd Alla, E.-S.M.; El-Badawy, S.M. Rheological properties and aging performance of sulfur extended asphalt modified with recycled polyethylene waste. *Constr. Build. Mater.* **2021**, *273*, 121771. [[CrossRef](#)]